Cancer Imaging (2012) **12,** 253–258
DOI: 10.1102/1470-7330.2012.0029

CI

e-med
www.e-med.org.uk

CASE REPORT

Imaging features of primary extranodal histiocytic sarcoma: report of two cases and a review of the literature

Sachin Shyamsunder Saboo, Katherine M. Krajewski, Atul B. Shinagare, Jyothi P. Jagannathan, Jason L. Hornick, Nikhil Ramaiya

Dana Farber Cancer Institute, 44 Binney Street, Boston, MA 02145, USA

Corresponding address: Sachin Shyamsunder Saboo, Department of Radiology, Dana Farber Cancer Institute, 44 Binney Street, Boston, MA 02145, USA.
Email: ssaboo@partners.org

Date accepted for publication 28 May 2012

Abstract

Histiocytic sarcoma is an extremely rare and aggressive malignancy of bone marrow origin that occurs in lymph nodes, skin, and the gastrointestinal tract. We report on the imaging features of two cases of primary histiocytic sarcoma, one in the retroperitoneum causing a tumor–bowel fistula and another with primary bone involvement.

Keywords: *Histiocytic sarcoma; MRI; CT; [^{18}F]FDG-PET/CT.*

Introduction

Histiocytic sarcoma (HS) is an extremely rare and aggressive hematopoietic malignancy of monocyte/macrophage lineage that occurs in lymph nodes, skin, and the gastrointestinal tract[1]. Although several series and individual cases of HS have been reported, the radiologic findings and complications of histiocytic sarcoma have rarely been described[2–4]. We report on the imaging features of two histopathologically proven cases of HS, one in the retroperitoneum causing a tumor–bowel fistula and another with primary bone involvement. This report is a useful addition to the understanding of the imaging of the disease.

Case reports

Patient 1

A 59-year-old French woman with a history of smoldering multiple myeloma and systemic lupus erythematosus (SLE) was admitted to our hospital with right flank pain, poor appetite, weight loss and multiple bilateral palpable submandibular nodes. Computed tomography (CT) of the chest, abdomen and pelvis showed a large $8.1 \times 8.6 \times 5.2$ cm retroperitoneal mass encasing both renal arteries and aorta with effacement of the adjacent inferior vena cava (IVC) with multiple mildly enlarged portocaval and peripancreatic lymph nodes. Magnetic resonance imaging (MRI) of the abdomen (Fig. 1) revealed a large retroperitoneal mass causing partial effacement of the IVC, and partial encasement of the aorta and superior mesenteric artery (SMA). The mass appeared predominantly mildly hyperintense to muscle on T2-weighted images with heterogeneous enhancement on post-contrast T1-weighted images. Differential diagnosis included lymphoma, metastatic disease, and infectious causes. [^{18}F]Fluorodeoxyglucose (FDG)-positron emission tomography (PET)/CT (Fig. 2) revealed intense and heterogeneous FDG uptake with a standardized uptake value (SUV_{max}) of 28 within this large retroperitoneal mass. Mildly FDG-avid enlarged nodes were noted in both axillae (SUV_{max} 2.1), left external iliac, and left inguinal regions, which may have been reactive due to SLE or tumor involvement.

A biopsy of the retroperitoneal mass showed HS. Histologically, the tumor was composed of pleomorphic epithelioid cells with marked nuclear atypia and abundant eosinophilic cytoplasm, including multinucleated forms, admixed with small lymphocytes (Fig. 3A). By immunohistochemistry, the tumor cells were strongly positive for CD68, CD163, CD4, and CD45RO

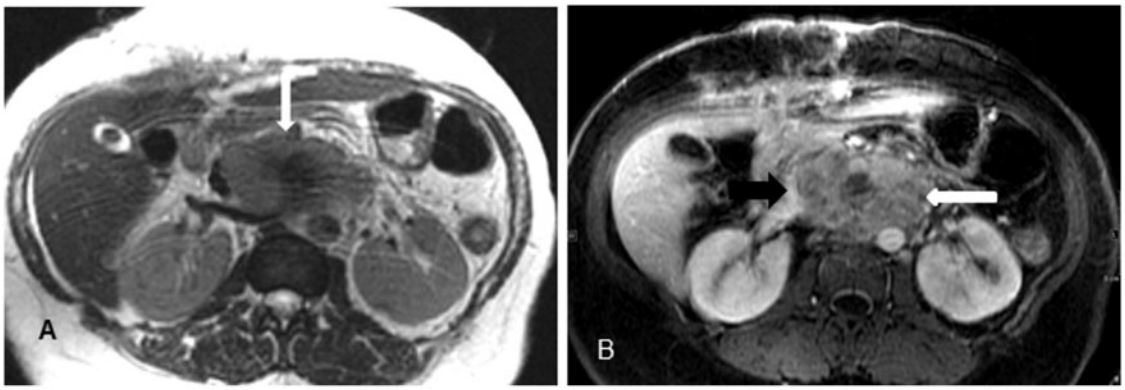

Figure 1 **(A) Axial T2-weighted and (B) axial T1 post-contrast gradient recalled echo (GRE) MRI images of the abdomen reveal a 8.1 × 8.6 × 5.2 cm retroperitoneal mass with central necrosis between the IVC and aorta (white arrows) causing partial effacement of the IVC (black arrow) and partial encasement of the aorta and SMA. The mass appeared predominantly mildly hyperintense to muscle on T2-weighted images with heterogeneous enhancement on post-contrast T1-weighted images. Note post laparotomy biopsy changes in the anterior abdominal wall in (B).**

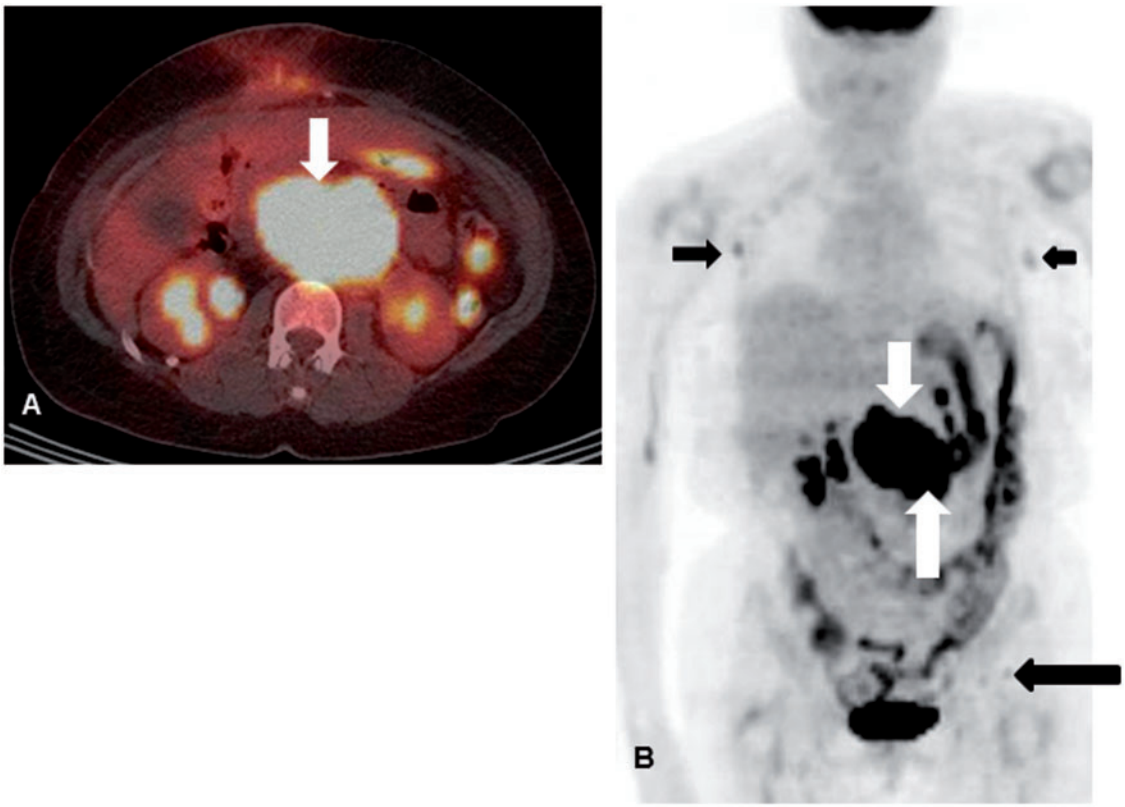

Figure 2 **(A) Axial fused PET/CT image and (B) coronal maximum intensity projection (MIP) image reveals intensely FDG-avid large retroperitoneal mass extending from the level of the SMA to a few centimeters above the aortic bifurcation. The mass shows intense and heterogeneous FDG uptake (white arrow) with SUV_{max} 28, with evidence of central necrosis. Mildly enlarged bilateral axillary (short black arrow) and left inguinal lymph nodes (long black arrow) with mild FDG uptake with SUV_{max} of 2.1 are also seen. Note relatively intense tracer uptake throughout the large bowel loops, due to the patient's use of metformin for diabetic control.**

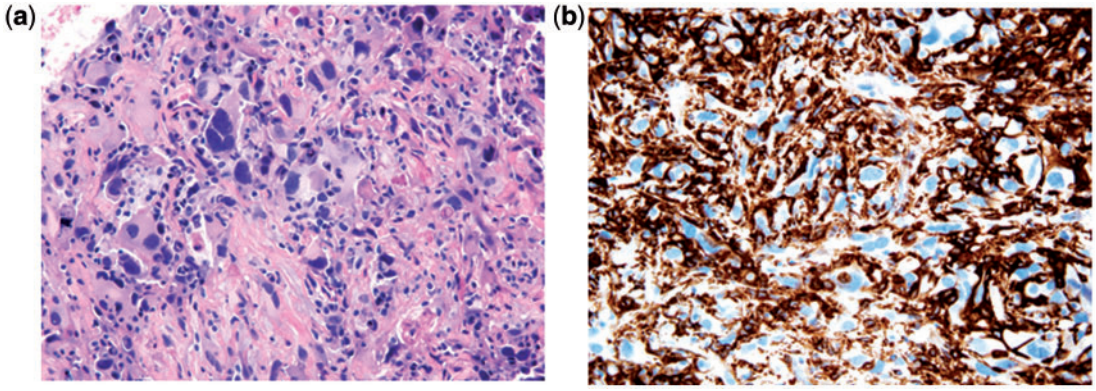

Figure 3 **(A) Core biopsy of the retroperitoneal mass from patient 1 showed a pleomorphic malignant neoplasm composed of epithelioid cells with eosinophilic cytoplasm and marked nuclear atypia, admixed with small lymphocytes. (B) Immunohistochemistry for CD163 showed strong membranous staining in the tumor cells, supporting the diagnosis of HS.**

Figure 4 **(A) Axial and (B) coronal, oral and intravenous contrast-enhanced CT scan of the abdomen reveals a large heterogeneously enhancing soft tissue mass (long white arrow) within the retroperitoneum at the level of the renal hila, measuring 9.2 × 6.8 × 11.2 cm. Oral contrast (black arrow) and air (short white arrow) is seen within the soft tissue mass, due to the fistula between the 3rd part of the duodenum and the retroperitoneal mass. The mass encases both renal arteries (not shown) and the aorta and causes effacement of the adjacent IVC (short black arrow).**

(Fig. 3B), whereas CD45 (LCA) and S100 protein were negative. These immunophenotypic features are typical of HS. Bone marrow aspiration and biopsy were unremarkable with no evidence of tumor involvement.

The patient was treated with cyclophosphamide, adriamycin, vincristine, and prednisone, followed by one cycle of local radiation therapy. However, 1 month later, she developed sharp abdominal pain in the periumbilical region with lower gastrointestinal bleeding and fever. CT scan of the abdomen (Fig. 4) revealed progression of the large heterogeneously enhancing retroperitoneal soft tissue mass with interval appearance of oral contrast and air within this mass, consistent with the development of a fistula between the mass and the 3rd portion of the duodenum. Radiation and chemotherapy were stopped due to increased risk of bacteremia secondary to the tumor–bowel fistula and underlying neutropenia. As the patient was not a surgical candidate, supportive care was administered. She died of HS 15 months after the initial presentation.

Patient 2

A 60-year-old man with a history of resection of incidentally detected grade 1 follicular lymphoma in a

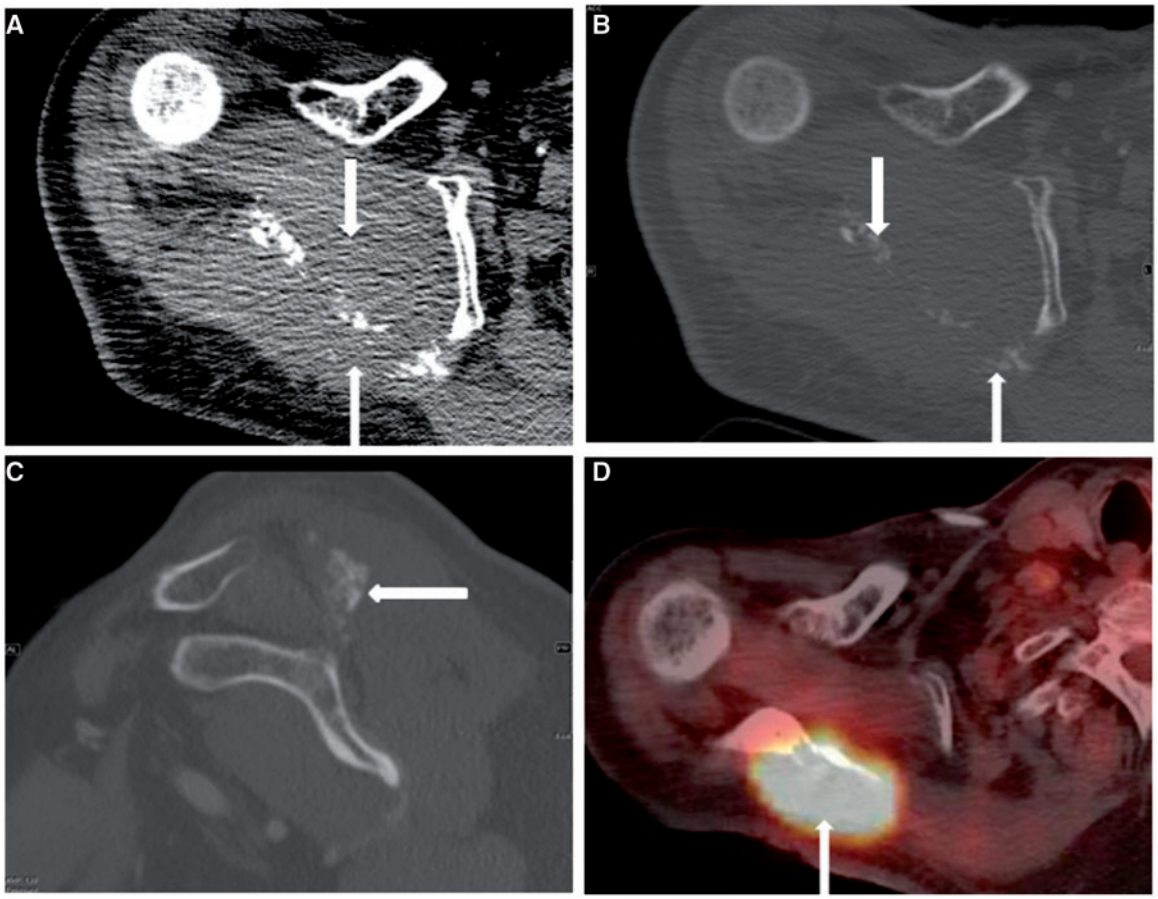

Figure 5 **CT scan of the right scapula with (A) axial soft tissue, (B) axial and (C) sagittal bone windows, reveals a large destructive mass lesion involving the posterior upper body of the scapula (arrows, A,B) and acromion (white arrow, C) with an associated large extraosseous soft tissue component. (D) Axial fused PET/CT image of the right scapula reveals intense FDG uptake (SUV_{max} 20) within the destructive scapular mass and extraosseous soft tissue component.**

mesenteric lymph node and a new FDG-avid mass lesion of the right posterior scapula presented to our hospital for further management of his persistent right scapular pain and mass, diagnosed as localized Langerhans cell histiocytosis at an outside institution. His outside pathology slides were reviewed and the diagnosis of HS of the right scapula was made. He had received 20 Gy of local radiation therapy, followed by two cycles of cyclophosphamide, adriamycin, vincristine, and prednisone (CHOP) at the outside hospital. Staging CT of the chest, abdomen and pelvis at our hospital showed a large destructive mass lesion involving the right posterior upper scapula and acromion with an associated large extraosseous soft tissue component (Fig. 5A–C). [^{18}F]FDG-PET/CT (Fig. 5D) revealed intense FDG uptake within the scapular mass with an SUV_{max} of 20. No other sites of FDG-avid disease were present. Repeat biopsy of the scapular mass was consistent with HS, showing a malignant neoplasm composed of sheets of epithelioid cells with coarse chromatin, voluminous pale cytoplasm (Fig. 6) and immunoreactivity for CD68, CD163 and S100. He received 50 Gy of local radiation therapy in 25 fractions for 2 months followed by three cycles of ifosphamide, carboplatin and etoposide (ICE) chemotherapy for the scapular mass without clinical response. He therefore underwent radical scapulectomy in January 2011 2 years after the initial presentation; however, he developed local recurrence at the skin incision site 1 month later, for which he was started on lenalidomide. However, due to progression of recurrent tumor, the patient opted for palliative care.

Discussion

HS (formerly known as true histiocytic lymphoma) is an extremely rare and aggressive malignancy of hematopoietic origin that may occur at any anatomic site. Although adult men are most commonly affected, no age group is exempt[1,5]. It presents with fever, night sweats, palpable adenopathy or local pain[1,5,6]. The most common primary sites of involvement include lymph nodes, and extranodal sites such as the skin and gastrointestinal tract; the central nervous system, spleen, bone marrow, and thyroid are rare sites of involvement[1,2,6,7]. HS may

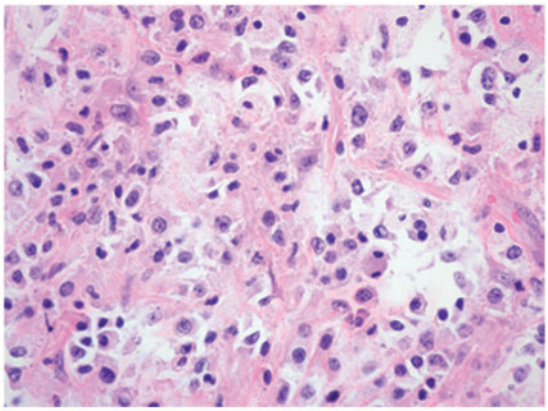

Figure 6 **Biopsy of the scapula mass from patient 2 showed a malignant neoplasm composed of sheets of epithelioid cells with coarse chromatin and abundant pale cytoplasm, consistent with HS.**

present as systemic disease involving multiple sites, also known as malignant histiocytosis[1,6].

HS is diagnosed on the basis of characteristic histologic features (usually sheets of large epithelioid cells with abundant palely eosinophilic cytoplasm) and supportive immunohistochemistry. However, many tumors previously diagnosed as HS before the development of specific immunohistochemical markers are now recognized to represent non-Hodgkin lymphomas, especially diffuse large B-cell lymphoma (DLBCL) and anaplastic large cell lymphoma (ALCL)[1,6]. The best available immunohistochemical markers for HS are CD163 and CD68[1,2,6].

Our first patient had a history of multiple myeloma and the second patient had concurrent follicular lymphoma; similar findings have been previously reported with concurrent or secondary development of HS in patients with follicular lymphoma[7,8], and an association with myelodysplasia[2,9].

Although previous studies have reported the clinical and pathologic findings of HS, its radiologic findings along with its complications have rarely been described. Imaging findings of HS are non-specific and depend on the site of involvement[3,4]. Imaging appearances of HS involving lymph nodes on [^{18}F]FDG-PET/CT have been previously reported in a few case reports[3,4,6,10] as intensely FDG-avid masses with SUV_{max} ranging from 12 to 23. According to the literature[4], high FDG uptake is seen in lesions of histiocytic origin, likely accounting for the high FDG uptake seen in this case.

In general, tumor–bowel fistula can occur secondary to aggressive local tumor progression, radiation therapy, infection, or due to antiangiogenic agents[11]. Retroperitoneal HS with tumor–bowel fistula in our first patient could be due to a combination of tumor progression and radiation therapy. Osseous involvement by HS appears as a destructive bone lesion with an extraosseous soft tissue component[12]. Malignant histiocytosis on imaging can manifest as hepatosplenomegaly, multifocal FDG-avid disease involving lymph nodes, liver, spleen, kidney and bone[10]. The differential diagnosis of HS on imaging, irrespective of the primary site is wide and includes large cell non-Hodgkin lymphomas (DLBCL and ALCL), metastatic carcinoma, metastatic melanoma, soft tissue sarcomas and infectious disease. In view of the high FDG uptake, lesions of fibroblastic or neurogenic origin should also be considered in the differential diagnosis[4]. Histologic examination and an appropriate panel of immunohistochemical markers permit differentiation between these possibilities[1,2,6].

HS may recur locally or metastasize to distant sites; commonly reported secondary sites include lymph nodes, lung, liver and bones[1,10]. Our patients did not have distant metastases. HS often presents at an advanced clinical stage with aggressive clinical course, poor response to chemotherapy and a high mortality rate[1–3]. Usually, there is less than a 2-year interval to death in most patients who die of HS[1]. These reported findings explain the rapid progression and death of our first patient and early recurrence in our second patient. However, rare cases presenting with clinically localized disease and smaller tumor size may have a favorable long-term outcome[1].

Treatment

There is no standard treatment protocol for HS. Local surgical resection followed by local radiation therapy, and systemic chemotherapy are treatment options; however, limited success has been reported[5,6]. Combination chemotherapy with protocols similar to those used to treat malignant lymphoma have been attempted with variable results. Thalidomide, along with autologous or allogeneic stem cell transplant (SCT) has been recently shown to be of benefit for several patients with HS[6,13].

Conclusion

This report describes the imaging appearances of two cases of HS along with complications on CT, MRI and PET/CT. Although acute myeloid leukemia or large cell lymphoma are much more common in patients presenting with a new malignant neoplasm with a known history of a myelodysplastic syndrome or low-grade lymphoma, HS may rarely occur. Since HS is indistinguishable from other malignant tumors on imaging studies, accurate histologic diagnosis using immunohistochemistry remains crucial to facilitate appropriate management.

References

[1] Hornick JL, Jaffe ES, Fletcher CD. Extranodal histiocytic sarcoma: clinicopathologic analysis of 14 cases of a rare epithelioid malignancy. Am J Surg Pathol 2004; 28: 1133–1144. doi:10.1097/01.pas.0000131541.95394.23. PMid:15316312.

[2] Sohn BS, Kim T, Kim JE, et al. A case of histiocytic sarcoma presenting with primary bone marrow involvement. J Korean Med Sci 2010; 25: 313–316. doi:10.3346/jkms.2010.25.2.313. PMid:20119590.

[3] Makis W, Ciarallo A, Derbekyan V, Lisbona R. Histiocytic sarcoma involving lymph nodes: imaging appearance on gallium-67 and F-18 FDG PET/CT. Clin Nucl Med 2011; 36: e37–e38. doi:10.1097/RLU.0b013e3182173979. PMid:21552013.

[4] Yaman E, Ozturk B, Erdem O, et al. Histiocytic sarcoma: PET-CT evaluation of a rare entity. Ann Nucl Med 2008; 22: 715–717. doi:10.1007/s12149-008-0175-7. PMid:18982475.

[5] Hayase E, Kurosawa M, Yonezumi M, Suzuki S, Suzuki H. Aggressive sporadic histiocytic sarcoma with immunoglobulin heavy chain gene rearrangement and t(14;18). Int J Hematol 2010; 92: 659–663. doi:10.1007/s12185-010-0704-8. PMid: 20976632.

[6] Gergis U, Dax H, Ritchie E, Marcus R, Wissa U, Orazi A. Autologous hematopoietic stem-cell transplantation in combination with thalidomide as treatment for histiocytic sarcoma: a case report and review of the literature. J Clin Oncol 2011; 29: e251–e253. doi:10.1200/JCO.2010.32.6603. PMid:21220616.

[7] Zhang D. Histiocytic sarcoma arising from lymphomas via transdifferentiation pathway during clonal evolution. Leuk Lymphoma 2010; 51: 739–740. doi:10.3109/10428191003774978. PMid: 20388055.

[8] Wang E, Papalas J, Hutchinson CB, et al. Sequential development of histiocytic sarcoma and diffuse large b-cell lymphoma in a patient with a remote history of follicular lymphoma with genotypic evidence of a clonal relationship: a divergent (bilineal) neoplastic transformation of an indolent B-cell lymphoma in a single individual. Am J Surg Pathol 2011; 35: 457–463. PMid:21317718.

[9] Pileri SA, Grogan TM, Harris NL, et al. Tumours of histiocytes and accessory dendritic cells: an immunohistochemical approach to classification from the International Lymphoma Study Group based on 61 cases. Histopathology 2002; 41: 1–29. doi:10.1046/j.1365-2559.2002.01418.x. PMid:12121233.

[10] Mori M, Matsushita A, Takiuchi Y, et al. Histiocytic sarcoma and underlying chronic myelomonocytic leukemia: a proposal for the developmental classification of histiocytic sarcoma. Int J Hematol 2010; 92: 168–173. doi:10.1007/s12185-010-0603-z. PMid:20535595.

[11] Chow H, Jung A, Talbott J, Lin AM, Daud AI, Coakley FV. Tumor fistulization associated with targeted therapy: computed tomographic findings and clinical consequences. J Comput Assist Tomogr 2011; 35: 86–90. doi:10.1097/RCT.0b013e3181fce2cb. PMid:21245693.

[12] Kaushal R, Jambhekar NA, Rao S, et al. Primary extranodal histiocytic sarcoma of lumbar spine. Skeletal Radiol 2012; 41: 231–235. doi:10.1007/s00256-011-1228-x. PMid:21786088.

[13] Abidi MH, Tove I, Ibrahim RB, Maria D, Peres E. Thalidomide for the treatment of histiocytic sarcoma after hematopoietic stem cell transplant. Am J Hematol 2007; 82: 932–933. doi:10.1002/ajh.20913. PMid:17617785.